Energy & Environmental Science

PAPER

Light trapping in photonic crystals

Cite this: *Energy Environ. Sci.*, 2014, **7**, 2725

Ken Xingze Wang,[ab] Zongfu Yu,[bc] Victor Liu,[bd] Aaswath Raman,[b] Yi Cui[ef] and Shanhui Fan*[b]

Received 14th March 2014
Accepted 30th May 2014

DOI: 10.1039/c4ee00839a

www.rsc.org/ees

We consider light trapping in photonic crystals in the weak material absorption limit. Using a rigorous electromagnetic approach, we show that the upper bound on the angle-integrated absorption enhancement by light trapping is proportional to the photonic density of states. The tight bound can be reached if all the states supported by the structure are coupled to external radiation. Numerical simulations are used to illustrate the theory and the design of both two- and three-dimensional photonic crystals for the purpose of light trapping. Using the van Hove singularities, the angle-integrated absorption enhancement in two-dimensional photonic crystals could surpass the conventional limit over substantial bandwidths.

Broader context

Commercial solar cells use light trapping to maximize solar absorption in the absorbing layers for improved efficiency and reduced cost. The upper limit of the absorption enhancement due to light trapping is $4n^2$, where n is the refractive index of the absorbing semiconductor, according to ray optics. This limit could be surpassed in nanostructured solar cells, however, typically only for limited bandwidths and incident angular ranges in any high-index absorbing semiconductor such as crystalline silicon. For broadband and omnidirectional absorption enhancement beyond $4n^2$ with large n, one promising candidate for the nanostructures is the photonic crystal in which the density of optical states could be significantly engineered. Using wave optics, we show that the upper limit of the angle-integrated light trapping absorption enhancement is proportional to the density of states in any given structure. To fully exploit the benefits of an elevated density of states, one needs to consider electromagnetic mode overlap and mode coupling in the structure, as well as the restrictions on the density of states engineering, among yet many other practical considerations. Our work envisions the theoretical possibility and provides the design guidelines of photonic crystal absorbers beyond the conventional limits by means of nanophotonic light trapping.

1 Introduction

Photon management strategies, including light trapping, have been tremendously successful in efficiency improvement and cost reduction in practical solar cells.[1,2] With the emergence of nanotechnology and the ability of molding the flow of photons, significant research efforts also focus on the tailoring and enhancement of sunlight absorption at a nanoscale, for the improvement of both short-circuit current and open-circuit voltage.[3–24]

In the vast majority of previous studies on light trapping, one considers a structure that includes a uniform layer of absorbing material.[3–10] Light trapping is then accomplished either by introducing surface gratings,[5] or by placing additional scattering layers near the absorbing layer.[4] In practical crystalline silicon solar cell design, the uniform layer is a bulk silicon structure that is typically a few hundred microns thick.[25] In many recent research studies on solar cell light trapping, the uniform layer can be as thin as a single optical wavelength or even at a deep subwavelength scale.[4] In all these cases, it is known that the light trapping enhancement limit is related to the photonic density of states.[26] For a bulk silicon cell, this leads to the well known $4n^2$ limit,[27–29] also referred to as the Yablonovitch limit, the Lambertian limit, the ray-optic limit, the ergodic limit, the bulk limit, the classical limit, the traditional limit, or the conventional limit. For thin films, the $4n^2$ limit can be modified depending on the details of guided modes in the film.[4,30,31,35,36] In addition, it has been shown that an elevated local density of states is an important element for improved light trapping.[13,32,33] That description is consistent with our wave optics light trapping theory.[34] The local density of states describes the enhancement of absorption at a given spatial location of the structure. To account for the performance of a solar cell, one needs to integrate over all spatial points in the solar cell where absorption occurs. One thus needs to perform spatial integration of the local density of states, which leads to the density of states picture that we use in this paper.

[a]*Department of Applied Physics, Stanford University, Stanford, California 94305, USA*
[b]*Department of Electrical Engineering, Stanford University, Stanford, California 94305, USA. E-mail: shanhui@stanford.edu*
[c]*Department of Electrical and Computer Engineering, University of Wisconsin–Madison, Madison, Wisconsin 53706, USA*
[d]*Palo Alto Research Center (PARC), 3333 Coyote Hill Road, Palo Alto, California 94304, USA*
[e]*Department of Materials Science and Engineering, Stanford University, Stanford, California 94305, USA*
[f]*Stanford Institute for Materials and Energy Sciences, SLAC National Accelerator Laboratory, Menlo Park, California 94205, USA*

Given the importance of density of states in defining the light trapping limit, one naturally should look beyond the relatively simple uniform absorbing layer and consider more complex medium. In particular, the photonic crystal structure is known to be able to drastically influence the density of states,[37] and its ability of dispersion and density of states engineering has been extensively explored and applied to a wide range of applications.[38] However, while light trapping in an absorber consisting of photonic crystals has been considered before,[39–57] the connection between the density of states and the light trapping limit in a photonic crystal has not been explicitly established.

In this work, we quantitatively establish the connection between the absorption enhancement and the density of states, and use this relationship to guide photonic crystal absorber designs. To maximize the absorption by light trapping, one should aim at maximizing the number of accessible modes (used interchangeably with states and resonances) supported by an absorbing structure. Moreover, we show that to take full advantage of the benefit of the photonic density of states, one need to consider additional issues including accessibility to these photonic states, as well as the overlap of the photonic states with the absorber.

This paper is organized as follows: in Section 2, we briefly review both the ray-optic and the wave-optic theory of light trapping, and derive a direct correspondence between the angle-integrated absorption enhancement and the photonic density of states. In Section 3, we numerically study light trapping in several two-dimensional (2D) photonic crystal absorbers, and account for the numerical results using the theoretical understanding developed in Section 2, highlighting in particular the requirements to observe significant density of states effects for light trapping in photonic crystals. Finally, we discuss three-dimensional (3D) photonic crystals in Section 4 and conclude in Section 5.

2 Model systems and theoretical background

2.1 Model systems

The main aim of our paper is to highlight the unique physics of light trapping in photonic crystals. As an illustration of the model system, we consider the structure as shown in Fig. 1. The structure consists of a photonic crystal with a finite number of periods in a vertical direction, with a perfect mirror on its bottom and with light incident from the top. The crystal is assumed to be of infinite extent in the horizontal directions, and consists of periodic arrays of dielectric elements in air. The dielectric has a real part of refractive index of n, which is assumed to be frequency independent throughout the paper, and a weak absorber with a small absorption coefficient $\alpha \ll 1/d$ where d is the thickness of the structure. Throughout the entire paper we assume a weak absorbing material where single-pass absorption is negligible. Knowing the absorption enhancement factor in such a weak absorption limit, one can derive the enhancement factor where the single-pass absorption is no longer negligible.[58,59] Focusing on the weak absorption limit therefore allows us to focus on illustrating the most prominent effects of the density of states modification in photonic crystals on light trapping absorption enhancement.

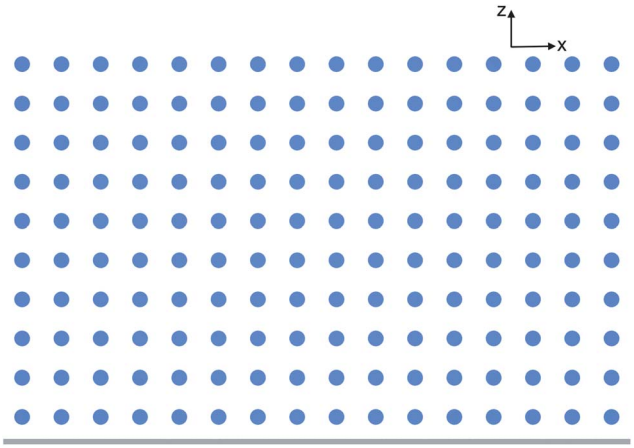

Fig. 1 A 2D photonic crystal structure consisting of a square lattice of dielectric rods in air. The radius of each rod is 0.2a, where a is the lattice constant. The dielectric constant of the rods, colored in blue, is 12, with an extremely small imaginary component. In the absorption simulations, the absorption is obtained through 10 layers of such rods with the other dimension being infinite and with a perfect mirror at the bottom. Light is incident on top. In the band structure and overlap factor calculations, the structure is treated as a lossless 2D photonic crystal infinite in both dimensions.

Real solar cells are of course 3D structures. To simplify numerical calculations, however, many theoretical studies on light trapping in solar cells have also considered 2D structures.[5,40,45,46,51,52] By 2D, we refer to structures that are uniform in a third dimension, and moreover we consider only light propagating within a 2D plane perpendicular to such third dimension. In this paper we consider both such 2D as well as 3D photonic crystals.

We will use numerical simulations to calculate the absorption of light in the configuration shown in Fig. 1. We will also contrast the numerical results from photonic crystals to corresponding uniform systems. The corresponding uniform systems (Fig. 2 and 3) consist of a uniform slab with the same refractive index n and absorption coefficient α as the dielectric in the photonic crystal in Fig. 1. The thickness of the uniform slab, d_{eff}, is chosen such that the amount of dielectric materials per unit area (in 3D) or unit length (in 2D) horizontally is the same as that of the photonic crystal systems. d_{eff} is therefore typically smaller than the physical thickness, d, of the photonic crystal. They are related by an area (in 2D) or volume (in 3D) fraction η:

$$d_{\text{eff}} = \eta d \tag{1}$$

In all our model or theory, the thickness of the photonic crystal is chosen or assumed such that d_{eff} is at least equal to a few wavelengths.

Fig. 2 A dielectric slab with flat surfaces. The thickness is equal to the equivalent thickness of the structure in Fig. 1 so the two structures contain the same amount of absorbing materials.

Fig. 3 A dielectric slab structure with a randomly textured front surface and a back mirror. The equivalent thickness is the same as in Fig. 2.

We consider two different corresponding uniform systems. Fig. 2 shows a slab where both the front and back surfaces are flat, with no mirror at the back surface. And we assume perfect antireflection for all frequencies and all angles on both surfaces. The absorption of light in such a slab defines the single-pass absorption, αd_{eff}, where $\alpha = 2k_0\text{Im}\{n\}$ is the absorption coefficient of the material, and k_0 is the wavevector of light in a vaccum and $\text{Im}\{n\}$ is the imaginary part of the refractive index.

The goal of any light trapping structure is to achieve absorption beyond such single-pass absorption, while keeping the same amount of the absorbing material. For such light trapping structures, in 3D, we define the absorption enhancement factor as

$$f(\omega,\theta,\varphi)=\frac{A(\omega,\theta,\varphi)}{\alpha d_{\text{eff}}} \tag{2}$$

Here, ω, θ, and φ are the frequency, the angle of incident light, and the polar angle of light, respectively. A is the absorption coefficient of the structure. There will not be a φ dependency in 2D.

The second corresponding uniform system represents the conventional light-trapping structure (Fig. 3), where one roughens the front surface of the uniform slab, and places a perfect mirror at the back. The limit of absorption enhancement in such a structure is very well understood, and will be briefly reviewed in Subsection 2.2. The comparison of the absorption of actual photonic crystal structures, to these two corresponding uniform systems, both of which are idealized, serves to highlight the physics and performance potential of photonic crystal light trapping schemes.

2.2 Ray-optic theory of light trapping

The ray-optic theory describes the conventional light-trapping structure (Fig. 3). In 3D, when the front surface is a Lambertian surface, one has the isotropic case where the absorption enhancement factor for light incident from any angle is the same, and is equal to $4n^2$.[28] This result is commonly referred to as the Yablonovitch or $4n^2$ limit. Here combining with the 2D results below, we refer all the ray-optic results as conventional limits. On the other hand, if the front surface is designed such that the structure can only accept light within a cone with an apex angle of θ, and moreover if one assumes that the enhancement factor is the same for all incident directions within that cone, one then has the anisotropic case where the absorption enhancement factor increases to $4n^2/\sin^2\theta$.[60,61]

Both the isotropic and the anisotropic cases above can be described in a unified fashion by defining an angle-integrated enhancement factor

$$F_{3\text{D}}(\omega)=\int_0^{\pi/2}\text{d}\theta\int_0^{2\pi}\text{d}\varphi f(\omega,\theta,\varphi)\cos\theta\sin\theta \tag{3}$$

where $f(\omega, \theta, \varphi)$ is defined in eqn (2) above. One can see that for both the isotropic and anisotropic cases we have $F_{3\text{D}} = 4\pi n^2$. Moreover, it has been shown that as an upper limit $F_{3\text{D}} = 4\pi n^2$ in fact applies to any light trapping structure of the form of Fig. 3 with an arbitrary angular response of $f(\theta, \varphi)$.[6]

Since no actual physical light trapping structure has an ideal isotropic angular response, to compare the performance of a physical light trapping structure to the conventional limit, it is imperative that one performs angle integration.[6,62] Observing an enhancement factor beyond $4n^2$ for a single angle of incidence, for example, should not be taken as the evidence that one has overcome the conventional limit.[63] In this context, the $4\pi n^2$ limit, which is really the conventional limit expressed in an angle-integrated fashion, is very useful when one needs to compare the performance of a physical structure to the ray-optic limit.

The ray-optic theory also describes the conventional light trapping structure of Fig. 3 in 2D. For the isotropic case the enhancement factor is

$$f(\omega,\theta)=\pi n \tag{4}$$

And the upper limit for the angle-integrated absorption enhancement factor is

$$F_{2\text{D}}(\omega)=\int_{-\pi/2}^{\pi/2}\text{d}\theta f(\omega,\theta)\cos\theta=2\pi n \tag{5}$$

which applies to isotropic as well as anisotropic cells in 2D. These 2D results are not nearly as well known as the original $4n^2$ limit in 3D, and moreover, to the best of our knowledge, were first derived using the wave-optic theory formalism.[5] Therefore below we provide a bit more details on the derivation of the πn limit for the 2D isotropic case using ray optics.

For a uniform 2D structure, it is straightforward to obtain a factor of n from the enhancement of light intensity and another factor of 2 from a back mirror, following the same approach as in the derivation of the $4n^2$ limit.[28] For an oblique ray at an angle θ, the path length is enhanced by $1/\cos\theta$. The angle-integrated enhancement of the path length is obtained by an angular integration over the individual path length enhancement, multiplied by a weighting factor that depends on the surface property and the dimension of the problem.[64] For a Lambertian surface, the weighting factor is $\cos\theta$ normalized by an angular integration over $\cos\theta$. Therefore, the average path length enhancement in 2D is

Table 1 Conventional light trapping limits in 2D and 3D for a single incidence angle and after angular integration. n is the refractive index of the weakly absorbing material

Dimension	Isotropic	Angle-integrated
2D	πn	$2\pi n$
3D	$4n^2$	$4\pi n^2$

$$\int_{-\pi/2}^{\pi/2} \mathrm{d}\theta \frac{1}{\cos\theta} \frac{\cos\theta}{\int_{-\pi/2}^{\pi/2} \mathrm{d}\theta \cos\theta} = \frac{\pi}{2} \quad (6)$$

instead of a factor of 2 in 3D. Multiplying the three enhancement factors, we obtain the πn enhancement for 2D light trapping.

The different versions of the conventional limits are summarized in Table 1.

2.3 Wave-optic theory of light trapping

For the same geometry in Fig. 3, the wave-optic light trapping theory could reproduce the ray-optic results in Table 1. In addition, the theory could account for more complex structures, including photonic crystals.

In the wave-optic theory, light trapping is described by the coupling of incident radiation into the optical modes supported by the structure. Absorption is enhanced through the aggregate contribution of these resonances. This physics can be captured by a statistical temporal coupled-mode theory.[4,5,65,66] We assume that the free space provides N planewave channels and that the absorbing structure supports M resonances. Each planewave channel could lead incoming radiation to each resonance, and each resonance could also leak to each planewave channel. The coupling between the m^{th} resonance to the planewaves with an incident wave from the n^{th} channel is described by the following temporal coupled-mode equation

$$\frac{\mathrm{d}}{\mathrm{d}t} a_m = \left(j\omega_m - \frac{\sum_{s=1}^{N} \gamma_{m,s} + \gamma_0}{2} \right) a_m + j\sqrt{\gamma_{m,n}} S_n \quad (7)$$

The resonance amplitude a_m is normalized such that $|a_m|^2$ is the electromagnetic energy stored in the resonant mode per unit area, and the incident planewave amplitude S_n is normalized such that $|S_n|^2$ corresponds to its intensity. ω_m is the resonant frequency of the m^{th} resonance. $\gamma_{m,s}$ is the loss rate from the m^{th} resonance to the s^{th} channel $\forall s \in \{1, 2, \ldots, N\}$. The loss rate is equal to the in-coupling rate by energy conservation and time-reversal symmetry. γ_0 is the loss rate of the resonance due to intrinsic material absorption.

In a uniform absorber of Fig. 3 whose thickness is sufficiently large so that the resonances completely overlap with the absorber in space, $\gamma_0 = \alpha c/n$. In a photonic crystal (for example, in Fig. 1), however, the overlap is generally less than unity.[38,67] We define Γ to be the overlap or confinement factor that characterizes the average overlap of the electric field with the weakly absorbing active material. Hence, the intrinsic loss rate is in general given by

$$\gamma_0 = \alpha \frac{c}{n} \Gamma \quad (8)$$

To rigorously derive eqn (8), we could treat the absorption as a perturbation to a transparent structure and integrate over the energy loss *versus* total energy throughout the entire space. This intrinsic loss rate modification generalizes the wave-optic light trapping theory over the earlier work.[6]

From eqn (7), we can calculate the broadband absorption enhancement by the m^{th} resonance when light is incident from the n^{th} channel. By summing over the contributions from all M resonances and N channels in the frequency range of $[\omega, \omega + \Delta\omega]$, and by comparing the absorption to the single-pass absorption αd_{eff}, we can calculate the angle-integrated absorption enhancement factor F, which in the k space translates into a summation over all the channels

$$F = \sum_n f_n = \frac{2\pi}{\alpha d_{\text{eff}} \Delta\omega} \sum_m \frac{\sum_n \gamma_{m,n}\gamma_0}{\sum_n \gamma_{m,n} + \gamma_0} \leq \frac{2\pi c \Gamma}{nd\eta} \rho(\omega) \quad (9)$$

where $\rho(\omega) = M/\Delta\omega$ is the spectral density of states, and f_n is the contribution to the enhancement factor from the n^{th} channel. η is the volume or area fraction of the absorbing material. The equality is approached if $\sum_{s=1}^{N} \gamma_{m,s} \gg \gamma_0$ for all m, that is, all the resonances are in the over-coupling regime. Since the material is weakly absorptive, the equality holds as long as all resonances are coupled to external radiation, in other words, all photonic states in the structure contribute to light trapping, and the averaging over a bandwidth results in the appearance of the density of states in the enhancement factor F.

Eqn (9) establishes a tight upper limit for absorption enhancement in light-trapping structures. In a bulk structure, $\Gamma = 1$, $\eta = 1$, the various versions of the conventional limit are readily reproduced by the theory (Table 1).[4–6] In particular, the information in oblique rays in the ray-optic picture is in essence captured by the coupling between resonances and channels in the wave-optic picture. If we assume that a resonance couples equally to all the channels, there will be a cosine factor in the intensity normalization, which is the same cosine factor for deriving the factor of 2 enhancement for a Lambertian surface. As a result, this factor of 2 lies implicitly in the wave-optic theory.[4]

2.4 Unique aspects of photonic crystals

The wave-optic theory in Subsection 2.3 points to several unique aspects of light trapping in photonic crystals. We examine the most prominent deviations of the optical properties of photonic crystals from those of bulk structures:

(1) The density of states of a photonic crystal (for example, in Fig. 1) can differ significantly from that of the bulk structure (for example, in Fig. 3).

(2) For a bulk structure, if its thickness is greater than a few wavelengths, one can assume complete overlap of the modes with the absorbing material. In contrast, in a photonic crystal, the electromagnetic fields do not completely overlap with the absorbing material, and therefore the modal absorption loss rate is related to crystal geometries as well as material constants.

(3) To access all the modes in a bulk structure, one typically employs surface roughness. In contrast, we will show that a photonic crystal by itself, with appropriate configurations, already provides complete access to all its modes even without surface disorders.

These aspects will be examined in detail in Section 3.

3 Detailed aspects of light trapping in 2D photonic crystals

3.1 Relevant aspects of the band structure of a 2D photonic crystal

As a model system, we start by considering a lossless and infinite 2D photonic crystal consisting of a square lattice of dielectric rods in air (Fig. 1). The radius of each rod is $r = 0.2a$, where a is the lattice constant. The dielectric material has a non-dispersive dielectric constant of 12, which is close to the value of silicon or gallium arsenide at optical frequencies.

We use the MPB (MIT Photonic-Bands) package to calculate the band structure.[68] In Fig. 4, we show the band structure of the photonic crystal along the line segments connecting the high symmetry points. There exist photonic bandgaps for the TM (transverse-magnetic) polarization, but not for the TE (transverse-electric) polarization. In order to highlight the features in the density of states of a 2D photonic crystal, we choose to work with the TM polarization for all subsequent discussions for 2D.

The same photonic band structure in Fig. 4 can alternatively be presented as a projected band diagram (Fig. 5), where we project the 2D band structure $\omega(k_x, k_z)$ onto the ω–k_x plane. The shaded regions in Fig. 5 correspond to states in the photonic crystal, the unshaded region is the gap region. We notice that a significant part of the first band and some parts of the second band lie below the light line $\omega = ck_x$. Such a projected band structure will be useful for the discussion of mode coupling issues in Subsection 3.5.

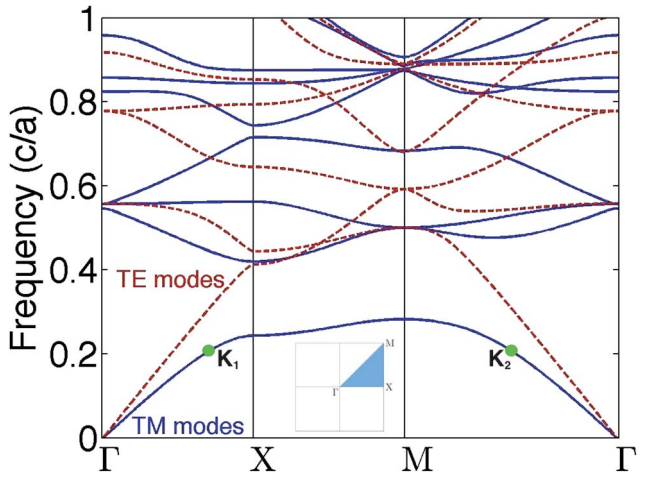

Fig. 4 Band structure of the photonic crystal in Fig. 1. The first Brillouin zone of the square lattice is shown in the inset. Γ denotes the k point (0, 0), X denotes (0, π/a), and M denotes (π/a, π/a).

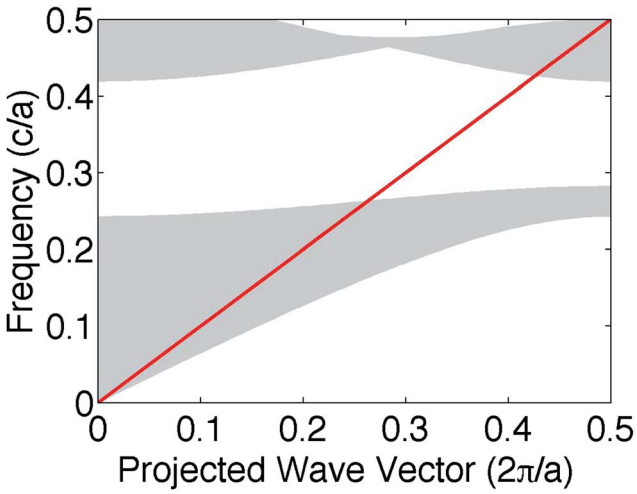

Fig. 5 Projected TM band structure obtained from Fig. 4. The lightline is given by $\omega = ck_x$, where k_x is the projected wave vector.

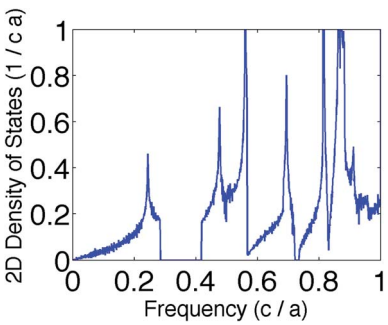

Fig. 6 Density of TM states per area for the 2D photonic crystal in Fig. 1.

We can calculate the density of states of this photonic crystal by a uniform sampling of all the k-points in the first Brillouin zone. In Fig. 6, we observe two bandgaps at frequencies close to $0.3c/a$ and $0.7c/a$, as well as a number of van Hove singularities where the density of states is divergent.[69,70] The van Hove singularities will be discussed in Subsection 3.3, and the low frequency limit will be discussed in Subsection 3.4.

For each mode, we can also calculate the overlap factor Γ between the electric field and the dielectric rods using the DtN (Dirichlet-to-Neumann) method.[71] At any given frequency, we select two k points from the segments connecting Γ to X to M and back to Γ. The selected k points correspond to the two leftmost intersections of horizontal cuts with the band structure plot in Fig. 4. Fig. 7 shows the overlap factors for such two k points for a range of frequencies. We observe that, at each frequency, the modes at different k points tend to have very

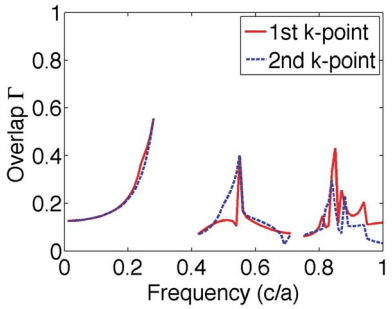

Fig. 7 Overlap factor of the TM mode for two selected k points at each frequency. The k points are selected from left to right, for example, at a frequency of $0.2c/a$, the first two k points are shown as K_1 and K_2, in Fig. 4. Inside the bandgap, the overlap factor is not defined.

similar overlap factors. In the limiting case at zero frequency, the field becomes uniform, and the overlap factors approach the area fraction $\eta = \pi r^2/a^2 \approx 0.126$. The first and second bands have quite different overlap factors, which can be explained by the variational theorem.[38] The first band tends to concentrate more of its electromagnetic energy in the dielectric, hence the overlap factors are higher than the area fraction η. Within the first band, there is an increase in overlap factors with respect to frequency, following the trend in the density of states. Γ is not defined in the photonic bandgaps, where light propagation and absorption are forbidden.

3.2 Absorption enhancement factor in the 2D photonic crystal and comparison to the density of states

We calculate the absorption in a lossy and finite version of the 2D photonic crystal considered in Subsection 3.1, as shown in Fig. 1. The crystal contains a finite number of periods in a vertical direction, with a perfect mirror on its bottom and with light incident from the top. The crystal is assumed to be of infinite extent in the horizontal directions. In the numerical simulations, we choose an extremely weak attenuation coefficient $\alpha = 10^{-8}/d$, and this particular numerical value cancels out after taking the ratio between the calculated absorption and the single-pass absorption as defined in eqn (2). The 2D photonic crystal contains 10 layers in the normal direction of incident light. Because the absorption is weak and there are a sufficient number of layers, the density of states and overlap factors can be well approximated by those calculated in Subsection 3.1 for the corresponding lossless and infinite photonic crystal.

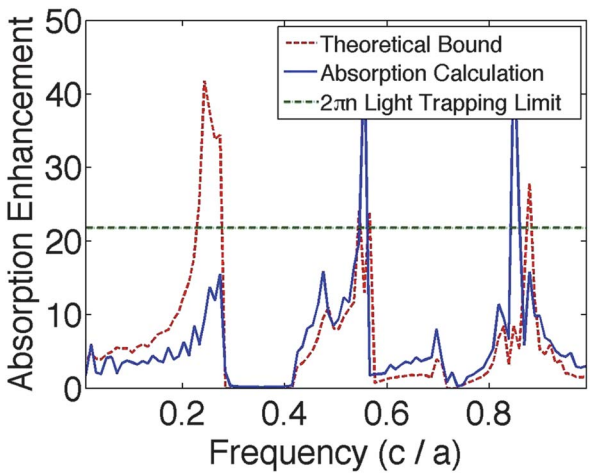

Fig. 8 Comparison of the angle-integrated light trapping absorption enhancement factor and its theoretical upper bound for the 2D photonic crystal in Fig. 1.

We calculate the absorption enhancement factor $f(\theta)$ for the entire range of incident angles θ with the Fourier modal method using the S^4 (Stanford Stratified Structure Solver) package.[72] From $f(\omega, \theta)$, we obtain the angle-integrated absorption enhancement factor F_{2D} using eqn (5). Numerically, we observe that F_{2D} is not influenced by the choice of the number of layers as long as the number is sufficiently large. We plot F_{2D} in Fig. 8 and compare it with both the density of states bound given by eqn (9) and the conventional limit of $2\pi n$.

To calculate the density of states bound on the right hand side in eqn (9), we first convert the summation in the real space as an angular integration in 2D to a summation over channels in the wave vector space. The 2D angle-integrated absorption enhancement factor can be written as

$$F_{2D} = \int_{-\pi/2}^{\pi/2} \mathrm{d}\theta f(\theta)\cos\theta = \frac{1}{k_0}\int_{|k_x|<k_0} \mathrm{d}k_x f(k_x) \quad (10)$$

$$= \frac{\Delta k}{k_0}\sum_n f_n \quad (11)$$

where θ is the angle of incidence and

$$k_x = k_0 \sin\theta$$

$$k_0 = \frac{\omega}{c}$$

$$\Delta k = \frac{2\pi}{L}$$

where L is the lattice constant of the photonic crystal or an artificially imposed periodicity of a bulk structure. Using eqn (9) and 11, we obtain

$$F_{2D} \le \frac{(2\pi c)^2 \Gamma}{n\eta\omega}\rho_{2D}(\omega) \quad (12)$$

where $\rho_{2D}(\omega)$ is the density of states per unit area.

In Subsection 3.1, we calculate $\rho_{2D}(\omega)$ (Fig. 6), as well as $\Gamma(\omega)$ (Fig. 7) for selected k points. Since the overlap factors Γ are approximately equal for different k points at the same frequency, we simply take an average of the two overlap factors shown in Fig. 7, and use the average overlap factor Γ in eqn (12). With this information and other parameters of the structure, we can obtain the right hand side expression $(2\pi c)^2\Gamma\rho_{2D}(\omega)/n\eta\omega$ of

eqn (12), which gives an upper bound for F_{2D}. We plot this bound for a range of frequencies in Fig. 8, referring to it as the "Theoretical Bound" curve.

Fig. 8 verifies our theoretical result on the correspondence between the absorption enhancement and the theoretical bound, we note in particular the following aspects:

(1) At a few narrow ranges of frequencies, the Yablonovitch limit is surpassed due to the van Hove singularities in the photonic density of states. We discuss this further in Subsection 3.3.

(2) Overall the absorption enhancement is below the conventional limit. We explain this with an effective medium argument in Subsection 3.4.

(3) The photonic crystal absorber, without gratings or surface roughness, is itself a very efficient scatterer. In most frequency ranges above $0.3c/a$, there is a close match between the density of states and the absorption curves, implying that most accessible resonances are excited. Unlike the conventional case of a uniform slab, there is no need to design surface gratings to achieve light trapping for photonic crystals. However, on the other hand, for the first band at a frequency from 0 to approximately $0.3c/a$, the numerically obtained light trapping absorption enhancement is significantly lower than its upper bound imposed by the density of states. This is because many modes are below the lightline and decoupled from external radiation, as we have alluded to in the discussion of Fig. 5. In Subsection 3.5, we investigate this aspect of mode coupling.

3.3 van Hove singularities in the density of states

We could engineer the photonic crystals and take advantage of the van Hove singularities in the density of states.[70] For practical applications, we might be able to apply the narrowband divergence of the density of states to achieve a strong absorption improvement, for example, at the bandedge in crystalline silicon where light trapping is crucial.[5,15]

van Hove singularities are generally more prominent in lower dimensions.[70] In fact, the density of states can diverge in 2D (Fig. 6, for example) while only its derivative can diverge in 3D (Fig. 16, for example). As a result, in 2D, the angle-integrated absorption enhancement factor indeed surpasses the Yablonovitch limit at van Hove singularities (Fig. 8), however, in 3D, a similar absorption enhancement is much more difficult to achieve, as we will show in Section 4.

The van Hove singularities in some sense redistribute the optical properties of photonic crystals.[73] For real materials, redistribution of the density of states is constrained by the density of states sum rule,[74,75] which implies that the increase in the density of states in one frequency region needs to be compensated by the decrease in other frequency regions, limiting the bandwidth and magnitude of the van Hove singularities. In this photonic crystal, the theoretical bound exceeds the conventional limit in the frequency range approximately from $0.22c/a$ to $0.27c/a$, due to the van Hove singularity in the density of states. Assuming that the frequency range is centered at a free space wavelength of 1000 nm, this frequency range then corresponds to a wavelength range of 907 nm to 1114 nm. Therefore, it is possible to use van Hove singularities to achieve a light trapping limit above the conventional limit over a bandwidth that is relevant for solar cell light trapping at the crystalline silicon bandedge. We may also stack multiple photonic crystals to use multiple van Hove singularities for an even broader bandwidth of light trapping absorption enhancement.

3.4 Long wavelength limit

We observe that away from the van Hove singularities, the absorption enhancement factor in a photonic crystal is in general lower than the $2\pi n$ limit. This is partly due to the fact that the overlap factor Γ is less than the area or volume fraction, and, more importantly, due to the lower effective density of states of the photonic crystal (Fig. 1) compared to the density of states in the bulk structure (Fig. 3). In this subsection, we use the effective medium theory,[38] which is accurate in the long wavelength limit, to provide a more in depth discussion of the density of states.

In the long wavelength (low frequency) limit, the light does not probe the fine details of the photonic crystal.[76] At low frequencies in Fig. 6, the density of states of the 2D photonic crystal is linear with respect to frequency, which follows the form of the density of states in a homogeneous dielectric material in 2D. In the long wavelength limit, we can therefore estimate the density of states of the photonic crystal treating it as a homogeneous effective medium and using the effective dielectric constant of such an effective medium. In general, construction of a composite material from two constituents with dielectric constants ε_1 and ε_2, and area or volume filling fractions of f_1 and f_2, respectively, is considered. The effective dielectric constant ε of the composite is then bounded as follows:[77–80]

$$(f_1{\varepsilon_1}^{-1} + f_2{\varepsilon_2}^{-1})^{-1} \leq \varepsilon \leq f_1\varepsilon_1 + f_2\varepsilon_2 \quad (13)$$

In 2D, imagine that we start with a bulk structure of weakly absorbing material with ε_1 and area A, and compare the structure to a photonic crystal structure for which we use the same amount of absorbing material with ε_1 but dilute it with a transparent material with ε_2 to a total area of A/η, where η is the area fraction of the absorbing material. Then $f_1 = \eta$ and $f_2 = 1 - \eta$.

The bound of light trapping enhancement in 2D, as pointed out in eqn (12), is related to the density of states $\rho(\omega)$, as well as the area fraction η and the overlap factor Γ. Since the overlap factor $\Gamma \approx \eta$ under the assumption that the electric field is distributed uniformly in space, the area fraction η and the overlap factor Γ cancel out in eqn (12), and the bound of light trapping enhancement is approximately proportional to $\rho(\omega)$. Furthermore, the 2D density of states is proportional to n^2 or ε:

$$\rho_{2D}(\omega) = \frac{4\varepsilon\omega}{\pi c^2} \quad (14)$$

We further assume that all modes are accessible, which can be made possible by methods discussed in Subsection 3.5.

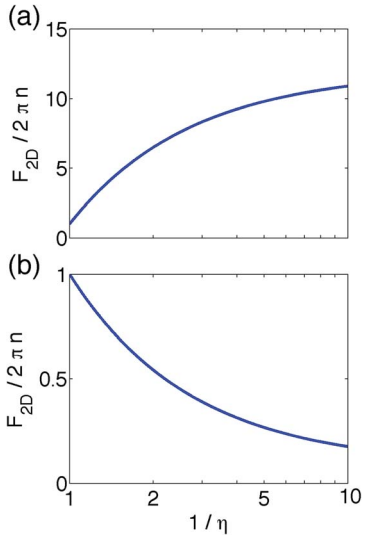

Fig. 9 Upper bounds of 2D angle-integrated absorption enhancement factors by eqn (15). η is the area fraction of the absorber whose index is n. (a) $\varepsilon_2/\varepsilon_1 = 12$. (b) $\varepsilon_1/\varepsilon_2 = 12$.

Using eqn (13) and 14, the upper bound of the angle-integrated light trapping enhancement factor $F_{2D}/2\pi n$, where $n = \sqrt{\varepsilon_1}$, is then given by

$$\frac{F_{2D}}{2\pi n} \leq \eta + (1-\eta)\frac{\varepsilon_2}{\varepsilon_1} \tag{15}$$

In Fig. 9, we plot this upper bound in eqn (15) as a function of the area fraction η of the absorbing material. In Fig. 9(a) we consider the hypothetical case where the absorbing material has a low dielectric constant ε_1, and is embedded in a transparent background of a high dielectric constant with $\varepsilon_2 = 12\varepsilon_1$. In this case, $F_{2D}/2\pi n$ significantly exceeds unity, indicating that such a structure has a light trapping potential that is significantly above conventional light trapping with the same absorbing material forming a uniform bulk. This effect was noted in ref. 4 and is due to the enhanced density of states from the high index dielectric material at the background.

In Fig. 9(b), we consider the more typical case, where the absorbing material has a high dielectric constant $\varepsilon_1 = 12$, and is embedded in a transparent background of a low dielectric constant $\varepsilon_2 = 1$. In this case, $F_{2D}/2\pi n$ is always less than unity. In other words, in the long wavelength limit, such a structure will always underperform, in terms of its light trapping capability, as compared to a uniform bulk absorbing medium with the same dielectric constant ε_1. The underperformance arises since the presence of the low index material significantly reduces the density of states of the overall structure. The theoretical results as illustrated in Fig. 9(b) are consistent with all numerical results presented in this paper. In particular, while the theoretical results are derived using the effective medium theory that strictly speaking is correct only in the long wavelength limit, all our numerical results indicate that away from the van Hove singularities, the photonic crystal structure that we examine in this paper has absorption enhancement that significantly underperforms the conventional limit for the corresponding uniform bulk medium. While the density of states away from the long wavelength limit certainly cannot be estimated from the effective medium theory, the overall trend, that the use of a low index material should reduce the average density of states, should in general be valid. This effect also limits the bandwidth over which the use of van Hove singularities can outperform the conventional limit, since it sets a lower floor for the enhancement factor away from the van Hove singularities.

Besides the considerations on light trapping, antireflection is also crucial for any practical solar cells.[15,81] In particular, optimal antireflection is a prerequisite for optimal light trapping.[59] In the examples we show in Subsection 3.2, although the density of states of the photonic crystal structure is lower than that of the bulk structure due to "dilution" of the active material, this dilution also lowers the effective refractive index of the photonic crystal structure and provides better optical impedance matching to the free space. This mechanism of antireflection adds another dimension to the optimization problem of designing photonic crystal absorbers.

3.5 Mode coupling

Eqn (9) provides a tight upper limit for the angle-integrated absorption enhancement factor F. The upper limit can be reached if all the modes are in the over-coupling regime. Since we have assumed that the single-pass absorption is weak, any mode that can couple to the external radiation is over-coupled. Therefore, to reach the upper limit one only needs to ensure that all modes can couple to external radiation. This is evident from Fig. 8, where the absorption enhancement is significantly lower than its limit given by eqn (9) in the first band, and the limit can be approximately reached for the second and higher bands. As we noted above, if the modes in the first band were able to couple to external radiation, the $2\pi n$ light trapping limit would be surpassed over a sizable bandwidth, approximately from $0.22c/a$ to $0.27c/a$ in Fig. 8, at the lowest van Hove singularity. Therefore, it is important to investigate possible methods that would lead to complete accessibility of all the modes.

For the structure shown in Fig. 1, the mode coupling aspect can be understood by considering the projected band diagram shown in Fig. 5. Only modes above the light line, that is, modes satisfying $\omega \geq ck_x$, can couple to external radiation. Since $k_x \in [0, \pi/a_x]$, where $a_x = a$ in this case is the periodicity of the truncated structure along the x direction, if follows that a significant number of modes below $\omega = 0.5\frac{2\pi c}{a}$, which includes a great portion of the first band and a small portion of the second band, cannot couple to external radiation and thus cannot contribute to light trapping. This effect is seen in Fig. 8, where in the frequency range of the first band, the numerically determined enhancement factor falls far below the theoretical bound of eqn (5), whereas the numerically determined enhancement factor agrees quite well with the theoretical bound in the upper bands.

For a bulk structure, efficient coupling can be achieved when the light rays are randomized by surface roughness, or when the

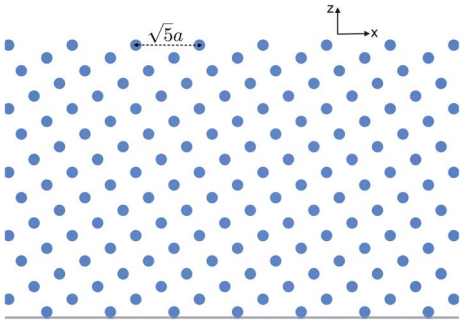

Fig. 10 A different truncation of the 2D photonic crystal in Fig. 1. The structure is rotated by 26.565° from the original structure in Fig. 1. The effective periodicity is $\sqrt{5}a$, where a is the lattice constant of the square lattice.

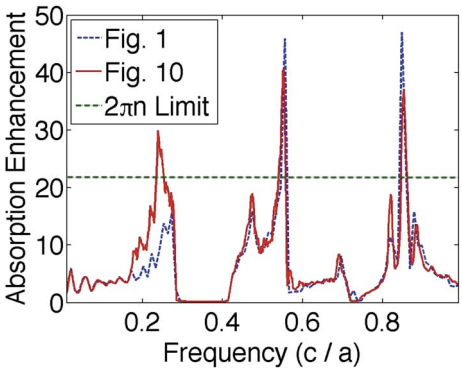

Fig. 11 Comparison of angle-integrated absorption enhancement spectra for the photonic crystals in Fig. 1 and 10.

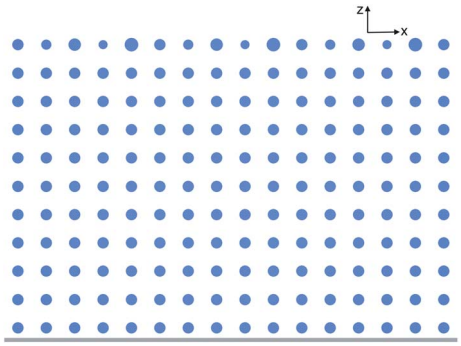

Fig. 12 The photonic crystal in Fig. 1 with one additional scattering layer on top. The dielectric rods in the first layer on top are transparent while the other rods are weakly absorptive. The real part of the dielectric constant is 12. The radius of each absorptive rod is 0.2a, where a is the lattice constant. The radii of the transparent rods are alternating in every five rods, being 0.2a, 0.18a, 0.22a, 0.16a, and 0.24a, thus forming a scattering layer.

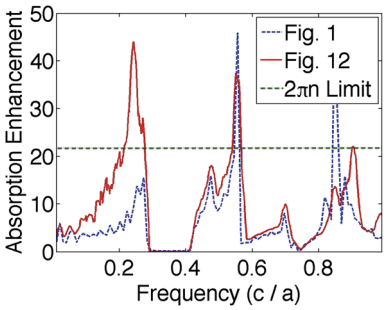

Fig. 13 Comparison of angle-integrated absorption enhancement spectra for the photonic crystals in Fig. 1 and 12.

light is scattered by a grating structure in which the periodicity is much larger than the wavelength of light.[5,6,82] The same underlying physics applies to photonic crystals in the wave-optic regime. In the following, we will explicitly demonstrate two simple methods to achieve complete coupling. Both methods seek to increase the spatial periodicity a_x of the truncated photonic crystal along the x direction.

In the first method, we simply choose a different crystal truncation. As an example, in Fig. 10 we choose the orientation of the crystal such that the periodicity along the surface $a_x = \sqrt{5}a$. In this case, one can show that all the modes in the crystal are above the light line. In the simulation results shown in Fig. 11, we indeed observe significant improvement of light trapping enhancement in the first band, as compared to the structure in Fig. 1. Also, the light trapping enhancement in the upper bands remains essentially unchanged as we vary the crystal orientation, as expected from the mode coupling argument.

In the second method, we add a layer of grating on top of the original structure. In Fig. 12, we reuse the structure from Fig. 1, but adding a top layer of transparent rods to keep d_{eff} unchanged. We vary the radii of the five transparent rods in that top layer, therefore creating random scattering of incoming light. Such a layer effectively increases the periodicity to 5a. In Fig. 13, we compare the light trapping enhancement without and with the random layer. Again, the second and higher bands are nearly identical, but, with the scattering, the absorption in the first band is vastly improved up to the theoretical bound given in eqn (12).

With either method, we are able to achieve nearly complete coupling of all the modes. Near the frequency range of the first van Hove singularity, roughly between 0.2c/a and 0.3c/a, the calculated light trapping absorption enhancement surpasses the conventional $2\pi n$ limit.

4 Brief discussion of light trapping in 3D photonic crystals

The formalism that we have developed for 2D systems can be readily extended to 3D. For example, in 3D, using eqn (9), the angle-integrated light trapping enhancement factor is

$$\begin{aligned} F_{3D} &= \int_0^{\pi/2} \mathrm{d}\theta \int_0^{2\pi} \mathrm{d}\varphi f(\theta,\varphi)\cos\theta\sin\theta \\ &= \frac{1}{{k_0}^2}\iint_{{k_x}^2+{k_y}^2\le {k_0}^2} \mathrm{d}k_x \mathrm{d}k_y f(k_x,k_y) \end{aligned} \tag{16}$$

$$= \frac{\Delta k^2}{{k_0}^2} \sum_n f_n \tag{17}$$

where θ is the incidence angle, and φ is the azimuthal angle, and

$$k_x = k_0 \sin\theta \cos\varphi$$

$$k_y = k_0 \sin\theta \sin\varphi$$

$$k_0 = \frac{\omega}{c}$$

$$\Delta k = \frac{2\pi}{L}$$

Similar to eqn (12), we have,

$$F_{3D} \leq \frac{(2\pi c)^3 \Gamma}{n\eta\omega^2} \rho_{3D}(\omega) \tag{18}$$

where $\rho_{3D}(\omega)$ is the density of states per unit volume.

Here, we highlight several notable differences between the 3D and 2D photonic crystals. In 3D, one can show that in the long wavelength limit, for a high index absorbing material embedded in a low index transparent background, the same index contrast and volume fraction would cause greater density of states reduction than in 2D. The result of the effective medium theory for this case gives

$$\frac{F_{3D}}{4\pi n^2} \leq \left[\eta + (1-\eta)\frac{\varepsilon_2}{\varepsilon_1}\right]^{\frac{3}{2}} \tag{19}$$

as plotted in Fig. 14(b) with $\varepsilon_1 = 12$ and $\varepsilon_2 = 1$. As a result, the absorption enhancement is significantly lower than the conventional limit of $4\pi n^2$ (Table 1). In addition, the van Hove singularities are much less prominent since the density of states at van Hove singularities is not divergent (although its derivative is divergent). Therefore, the angle-integrated light trapping enhancement factor does not exceed $4\pi n^2$, although at individual angles and wavelengths the $4n^2$ limit can be surpassed.

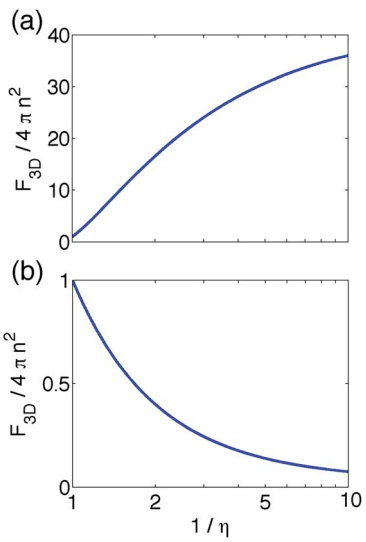

Fig. 14 Upper bounds of 3D angle-integrated absorption enhancement factors by eqn (19). η is the area fraction of the absorber whose index is n. (a) $\varepsilon_2/\varepsilon_1 = 12$. (b) $\varepsilon_1/\varepsilon_2 = 12$.

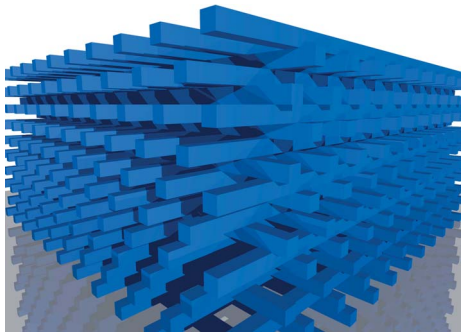

Fig. 15 3D photonic crystal. The woodpile structure consists of four alternating layers. Each layer has a thickness of 0.25*a* and consists of a 1D array of infinitely long square rods with widths of 0.25*a*, where *a* is the lattice constant. The horizontal locations of the first and the second layers are shifted laterally by 0.5*a* from the horizontal locations of the third and the fourth layers. The lattice orientations of the first and the third layers are orthogonal to the lattice orientations of the second and the fourth layers.

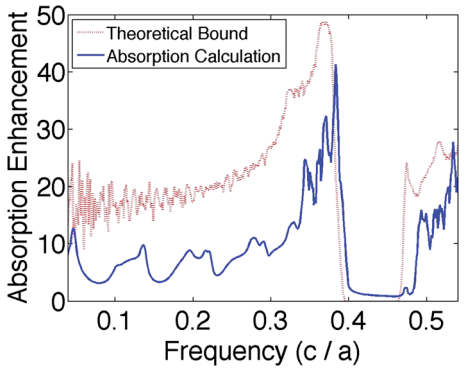

Fig. 16 Comparison of the angle-integrated absorption enhancement factor and its theoretical bound calculated by eqn (18) for the 3D woodpile structure in Fig. 15. The angle-integrated limit $4\pi n^2 = 150$.

We study a 3D woodpile structure,[83,84] consisting of the same dielectric with $\varepsilon = 12$ stacked in air as in the 2D simulations, as shown in Fig. 15. We obtain $\rho_{3D}(\omega)$ by MPB for an infinite and lossless structure, and F_{3D} by S^4 for the corresponding finite and lossy structure. We plot the right hand side expression $(2\pi c)^3\rho_{3D}(\omega)/n\omega^2$ in eqn (18) as the "Theoretical Bound" curve in Fig. 16, assuming that the overlap factor Γ is equal to the volume fraction η. We plot F_{3D} as the "Absorption Calculation" curve in Fig. 16. The absorption enhancement follows the density of states in the same manner as in the 2D case. We observe that both the theoretical bound and the actual angle-integrated absorption enhancement factor fall significantly below the conventional limit of $4\pi n^2 = 150$ in this case.

5 Conclusion

In this paper, we consider light trapping in photonic crystals, where the photonic crystals themselves operate as inhomogeneous absorbing media. We show that the density of states of photonic crystals strongly influences the light trapping behaviors. We also note the importance of modal overlap and the need for efficient mode coupling.

Our numerical results show that, in 2D, with the use of van Hove singularity in the density of states, the angle-integrated light trapping absorption enhancement factor can exceed the conventional limit over a substantial bandwidth. In 3D, it is more difficult to use photonic crystals to overcome the conventional limit, due to the weakening of the van Hove singularity and the fact that embedding a high index absorbing material in a low index background reduces the overall density of states away from van Hove singularities. These results provide a theoretical guidance for the design of optical absorbers that are inhomogeneous in general, including nanostructured photovoltaic and photoelectrochemical cells. We show that to design and experimentally realize high-efficiency photonic crystal solar cells, one should include the considerations on the effective medium, van Hove singularities, overlap factor, mode coupling, and antireflection. Photonic crystals can be and have been fabricated using a variety of techniques.[44,47,48,55,85–93]

Acknowledgements

This work is supported by the Department of Energy Grant no. DE-FG07ER46426, by the Bay Area Photovoltaic Consortium (BAPVC) funded under the Sunshot Initiative of US Department of Energy, and by the Center on Nanostructuring for Efficient Energy Conversion (CNEEC) at Stanford University, an Energy Frontier Research Center funded by the US Department of Energy, Office of Science and Office of Basic Energy Sciences under award number DE-SC0001060. The simulations were performed on the Extreme Science and Engineering Discovery Environment (XSEDE), which is supported by National Science Foundation grant number OCI-1053575.

References

1 N. Horiuchi, Towards highly efficient solar cells, *Nat. Photonics*, 2012, **6**, 136–137.
2 S. Mokkapati and K. R. Catchpole, Nanophotonic light trapping in solar cells, *J. Appl. Phys.*, 2012, **112**, 101101.
3 H. A. Atwater and A. Polman, Plasmonics for improved photovoltaic devices, *Nat. Mater.*, 2010, **9**, 205–213.
4 Z. Yu, A. Raman and S. Fan, Fundamental limit of nanophotonic light trapping in solar cells, *Proc. Natl. Acad. Sci. U. S. A.*, 2010, **107**, 17491–17496.
5 Z. Yu, A. Raman and S. Fan, Fundamental limit of light trapping in grating structures, *Opt. Express*, 2010, **10**, A366–A380.
6 Z. Yu and S. Fan, Angular constraint on light-trapping absorption enhancement in solar cells, *Appl. Phys. Lett.*, 2011, **98**, 011106.
7 X. Sheng, S. G. Johnson, J. Michel and L. C. Kimerling, Optimization-based design of surface textures for thin-film Si solar cells, *Opt. Express*, 2011, **19**, A841–A850.
8 A. Bozzola, M. Liscidini and L. C. Andreani, Photonic light-trapping *versus* Lambertian limits in thin film silicon solar cells with 1D and 2D periodic patterns, *Opt. Express*, 2012, **20**, A224.
9 J. G. Mutitu, S. Shi, C. Chen, T. Creazzo, A. Barnett, C. Honsberg and D. W. Prather, Thin film silicon solar cell design based on photonic crystal and diffractive grating structures, *Opt. Express*, 2008, **16**, 15238.
10 B. M. Wong and A. M. Morales, Enhanced photocurrent efficiency of a carbon nanotube p–n junction electromagnetically coupled to a photonic structure, *J. Phys. D: Appl. Phys.*, 2009, **42**, 055111.
11 A. Polman and H. A. Atwater, Photonic design principles for ultrahigh-efficiency photovoltaics, *Nat. Mater.*, 2012, **11**, 174.
12 J. N. Munday, The effect of photonic bandgap materials on the Shockley–Queisser limit, *J. Appl. Phys.*, 2012, **112**, 064501.
13 D. M. Callahan, J. N. Munday and H. A. Atwater, Solar cell light trapping beyond the ray optic limit, *Nano Lett.*, 2012, **12**, 214–218.
14 C. Battaglia, C.-M. Hsu, K. Söderström, J. Escarré, F.-J. Haug, M. Charrière, M. Boccard, M. Despeisse, D. T. L. Alexander, M. Cantoni, Y. Cui and C. Ballif, Light trapping in solar cells: can periodic beat random?, *ACS Nano*, 2012, **6**, 2790–2797.
15 K. X. Wang, Z. Yu, V. Liu, Y. Cui and S. Fan, Absorption enhancement in ultrathin crystalline silicon solar cells with antireflection and light-trapping nanocone gratings, *Nano Lett.*, 2012, **12**, 1616–1619.
16 S. Wang, B. D. Weil, Y. Li, K. X. Wang, E. Garnett, S. Fan and Y. Cui, Large-area free-standing ultrathin single-crystal silicon as processable materials, *Nano Lett.*, 2013, **13**, 4393–4398.
17 S. Sandhu, Z. Yu and S. Fan, Detailed balance analysis of nanophotonic solar cells, *Opt. Express*, 2013, **21**, 1209–1217.
18 C. Wang, S. Yu, W. Chen and C. Sun, Highly efficient light-trapping structure design inspired by natural evolution, *Sci. Rep.*, 2013, **3**, 1025.
19 V. K. Narasimhan and Y. Cui, Nanostructures for photon management in solar cells, *Nanophotonics*, 2013, **2**, 187–210.
20 S. Wiesendanger, M. Zilk, T. Pertsch, C. Rockstuhl and F. Lederer, Combining randomly textured surfaces and photonic crystals for the photon management in thin film microcrystalline silicon solar cells, *Opt. Express*, 2013, **21**, A450.
21 X. Sheng, L. Z. Broderick and L. C. Kimerling, Photonic crystal structures for light trapping in thin-film Si solar cells: Modeling, process and optimizations, *Opt. Commun.*, 2014, **314**, 41–47.
22 Z. Yu, S. Sandhu and S. Fan, Efficiency above the Shockley–Queisser limit by using nanophotonic effects to create multiple effective bandgaps with a single semiconductor, *Nano Lett.*, 2014, **14**, 66–70.

23 S. Eyderman, A. Deinega and S. John, Near perfect solar absorption in ultra-thin-film GaAs photonic crystals, *J. Mater. Chem. A*, 2014, **2**, 761.

24 T. Khaleque and R. Magnusson, Light management through guided-mode resonances in thin-film silicon solar cells, *J. Nanophotonics*, 2014, **8**, 083995.

25 M. A. Green, Silicon solar cells: state of the art, *Philos. Trans. R. Soc., A*, 2013, **371**, 20110413.

26 P. Sheng, A. N. Bloch and R. S. Stepleman, Wavelength-selective absorption enhancement in thin-film solar cells, *Appl. Phys. Lett.*, 1983, **43**, 579.

27 E. Yablonovitch and G. D. Cody, Intensity enhancement in textured optical sheets for solar cells, *IEEE Trans. Electron Devices*, 1982, **29**, 300.

28 E. Yablonovitch, Statistical ray optics, *J. Opt. Soc. Am.*, 1982, **72**, 899.

29 H. W. Deckman, C. B. Roxlo and E. Yablonovitch, Maximum statistical increase of optical absorption in textured semiconductor films, *Opt. Lett.*, 1983, **8**, 491.

30 M. Agrawal and P. Peumans, Broadband optical absorption enhancement through coherent light trapping in thin-film photovoltaic cells, *Opt. Express*, 2008, **16**, 5385–5396.

31 J. N. Munday, D. M. Callahan and H. A. Atwater, Light trapping beyond the $4n^2$ limit in thin waveguides, *Appl. Phys. Lett.*, 2012, **100**, 121121.

32 M.-Y. Shih, S. F. LeBoeuf, M. Pietrzykowski, O. V. Sulima, J. Rand, A. Davuluru, U. Rapol, L. Tsakalakos, J. Balch, P. J. Codella, B. A. Korevaar and J. Fronheiser, Strong broadband optical absorption in silicon nanowire films, *J. Nanophotonics*, 2007, **1**, 013552.

33 P. Wang and R. Menon, Optimization of generalized dielectric nanostructures for enhanced light trapping in thin-film photovoltaics via boosting the local density of optical states, *Opt. Express*, 2014, **22**, A99–A110.

34 M. L. Brongersma, Y. Cui and S. Fan, Light management for photovoltaics using high-index nanostructures, *Nat. Mater.*, 2014, **13**, 451.

35 H. R. Stuart and D. G. Hall, Thermodynamic limit to light trapping in thin planar structures, *J. Opt. Soc. Am. A*, 1997, **14**, 3001.

36 F.-J. Haug, K. Soderstrom, A. Naqavi and C. Ballif, Resonances and absorption enhancement in thin film silicon solar cells with periodic interface texture, *J. Appl. Phys.*, 2011, **109**, 084516.

37 R. C. McPhedran, L. C. Botten, J. McOrist, A. A. Asatryan and C. M. de Stereke, Density of states functions for photonic crystals, *Phys. Rev. E: Stat., Nonlinear, Soft Matter Phys.*, 2004, **69**, 016609.

38 J. D. Joannopoulos, S. G. Johnson, J. N. Winn and R. D. Meade, *Photonic Crystals: Molding the Flow of Light*, Princeton University Press, 2nd edn, 2008.

39 A. Mihi and H. Míguez, Origin of light-harvesting enhancement in colloidal-photonic-crystal-based dye-sensitized solar cells, *J. Phys. Chem. B*, 2005, **109**, 15968–15976.

40 A. Chutinan and S. John, Light trapping and absorption optimization in certain thin-film photonic crystal architectures, *Phys. Rev. A: At., Mol., Opt. Phys.*, 2008, **78**, 023825.

41 D. Duche, L. Escoubas, J.-J. Simon, P. Torchio, W. Vervisch and F. Flory, Slow Bloch modes for enhancing the absorption of light in thin films for photovoltaic cells, *Appl. Phys. Lett.*, 2008, **92**, 193310.

42 J. R. Tumbleston, D.-H. Ko, E. T. Samulski and R. Lopez, Electrophotonic enhancement of bulk heterojunction organic solar cells through photonic crystal photoactive layer, *Appl. Phys. Lett.*, 2009, **94**, 043305.

43 J. R. Tumbleston, D.-H. Ko, E. T. Samulski and R. Lopez, Absorption and quasiguided mode analysis of organic solar cells with photonic crystal photoactive layers, *Opt. Express*, 2009, **17**, 7670–7681.

44 D.-H. Ko, J. R. Tumbleston, L. Zhang, S. Williams, J. M. DeSimone, R. Lopez and E. T. Samulski, Photonic crystal geometry for organic solar cells, *Nano Lett.*, 2009, **9**, 2742–2746.

45 Y. Park, E. Drouard, O. E. Daif, X. Letartre, P. Viktorovitch, A. Fave, A. Kaminski, M. Lemiti and C. Seassal, Absorption enhancement using photonic crystals for silicon thin film solar cells, *Opt. Express*, 2009, **17**, 14312.

46 A. Chutinan, N. P. Kherani and S. Zukotynski, High-efficiency photonic crystal solar cell architecture, *Opt. Express*, 2009, **17**, 8871–8878.

47 S. Guldin, S. Hüttner, M. Kolle, M. E. Welland, P. Müller-Buschbaum, R. H. Friend, U. Steiner and N. Tétreault, Dye-sensitized solar cell based on a three-dimensional photonic crystal, *Nano Lett.*, 2010, **10**, 2303–2309.

48 S. B. Mallick, M. Agrawal, A. Wangerawong, E. S. Barnard, K. K. Singh, R. J. Visser, M. L. Brongersma and P. Peumans, Ultrathin crystalline-silicon solar cells with embedded photonic crystals, *Appl. Phys. Lett.*, 2012, **100**, 053113.

49 Q. G. Du, C. H. Kam, H. V. Demir, H. Y. Yu and X. W. Sun, Enhanced optical absorption in nanopatterned silicon thin films with a nano-cone-hole structure for photovoltaic applications, *Opt. Lett.*, 2011, **36**, 1713.

50 S. B. Mallick, M. Agrawal and P. Peumans, Optimal light trapping in ultra-thin photonic crystal crystalline silicon solar cells, *Opt. Express*, 2010, **18**, 5691.

51 D. Duche, E. Drouard, J.-J. Simon, L. Escoubas, P. Torchio, J. Le Rouzo and S. Vedraine, Light harvesting in organic solar cells, *Sol. Energy Mater. Sol. Cells*, 2011, **95**, S18–S25.

52 G. Gomard, X. Meng, E. Drouard, K. E. Hajjam, E. Gerelli, R. Peretti, A. Fave, R. Orobtchouk, M. Lemiti and C. Seassal, Light harvesting by planar photonic crystals in solar cells: the case of amorphous silicon, *J. Opt.*, 2012, **14**, 024011.

53 S. John, Why trap light?, *Nat. Mater.*, 2012, **11**, 997–999.

54 S. Eydeman, S. John and A. Deinega, Solar light trapping in slanted conical-pore photonic crystals: Beyond statistical ray trapping, *J. Appl. Phys.*, 2013, **113**, 154315.

55 P. Kuang, A. Deinega, M.-L. Hsieh, S. John and S.-Y. Lin, Light trapping and near-unity solar absorption in a three-dimensional photonic-crystal, *Opt. Lett.*, 2013, **38**, 4200.

56 K. Q. Le and S. John, Synergistic plasmonic and photonic crystal light-trapping: Architectures for optical up-conversion in thin-film solar cells, *Opt. Express*, 2014, **22**, A12.

57 A. Oskooki, Y. Tanaka and S. Noda, Tandem photonic-crystal thin films surpassing Lambertian light-trapping limit over broad bandwidth and angular range, *Appl. Phys. Lett.*, 2014, **104**, 091121.

58 M. A. Green, Lambertian light trapping in textured solar cells and light-emitting diodes: analytical solutions, *Prog. Photovolt. Res. Appl.*, 2002, **10**, 235–241.

59 Z. Yu, A. Raman and S. Fan, Thermodynamic upper bound on broadband light coupling with photonic structures, *Phys. Rev. Lett.*, 2012, **109**, 173901.

60 R. P. Patera and H. S. Robertson, Information theory and solar energy collection, *Appl. Opt.*, 1980, **19**, 2403–2407.

61 P. Campbell and M. A. Green, The limiting efficiency of silicon solar-cells under concentrated sunlight, *IEEE Trans. Electron Devices*, 1986, **33**, 234–239.

62 A. Naqavi, F.-J. Haug, K. Soderstrom, C. Battaglia, V. Paeder, T. Scharf, H. P. Herzig and C. Ballif, Angular behavior of the absorption limit in thin film silicon solar cells, *Prog. Photovolt. Res. Appl.*, 2013, DOI: 10.1002/pip.2371.

63 V. Ganapati, O. D. Miller and E. Yablonovitch, Light trapping textures designed by electromagnetic optimization for subwavelength thick solar cells, *IEEE Journal of Photovoltaics*, 2014, **4**, 175.

64 C. Battaglia, M. Boccard, F.-J. Haug and C. Ballif, Light trapping in solar cells: When does a Lambertian scatterer scatter Lambertianly?, *J. Appl. Phys.*, 2012, **112**, 094504.

65 H. A. Haus, *Waves the Fields in Optoelectronics*, Prentice-Hall, 1984.

66 S. Fan, W. Suh and J. D. Joannopoulos, Temporal coupled-mode theory for the Fano resonance in optical resonators, *J. Opt. Soc. Am. A*, 2003, **20**, 569.

67 A. Naqavi, F.-J. Haug, C. Battaglia, H. P. Herzig and C. Ballif, Light trapping in solar cells at the extreme coupling limit, *J. Opt. Soc. Am. B*, 2013, **30**, 13.

68 S. G. Johnson and J. D. Joannopoulos, Block-iterative frequency-domain methods for Maxwell's equations in a planewave basis, *Opt. Express*, 2001, **8**, 173–190.

69 L. Van Hove, The occurrence of singularities in the elastic frequency distribution of a crystal, *Phys. Rev.*, 1953, **89**, 1189–1193.

70 F. Bassani and G. P. Parravicini, *Electronic States and Optical Transitions in Solids*, Pergamon Press, 1975.

71 V. Liu and S. Fan, Efficient computation of equi-frequency surfaces and density of states in photonic crystals using Dirichlet-to-Neumann maps, *J. Opt. Soc. Am. B*, 2011, **28**, 1837–1843.

72 V. Liu and S. Fan, S^4: A free electromagnetic solver for layered periodic structures, *Comput. Phys. Commun.*, 2012, **183**, 2233–2244.

73 S. V. Gaponenko, *Introduction to Nanophotonics*, Cambridge University Press, 2010.

74 S. M. Barnett and R. Loudon, Sum rule for modified spontaneous emission rates, *Phys. Rev. Lett.*, 1996, **77**, 2444.

75 S. Scheel, Sum rule for local densities of states in absorbing dielectrics, *Phys. Rev. A: At., Mol., Opt. Phys.*, 2008, **78**, 013841.

76 C. Lin, C. Chen, A. Sharkawy, G. J. Schneider, S. Venkataraman and D. W. Prather, Efficient terahertz coupling lens based on planar photonic crystals on silicon on insulator, *Opt. Lett.*, 2005, **30**, 1330.

77 D. Bergman, The dielectric constant of a composite material – a problem in classical physics, *Phys. Rep.*, 1978, **43**, 377.

78 D. J. Bergman, Exactly solvable microscopic geometries and rigorous bounds for the complex dielectric constant of a two-component composite material, *Phys. Rev. Lett.*, 1980, **44**, 1285.

79 G. W. Milton, Bounds on the complex permittivity of a two component composite material, *J. Appl. Phys.*, 1981, **52**, 5286.

80 G. W. Milton, *The Theory of Composites*, Cambridge University Press, 2002.

81 H. K. Raut, V. A. Ganesh, A. S. Nair and S. Ramakrishna, Anti-reflective coatings: A critical, in-depth review, *Energy Environ. Sci.*, 2011, **4**, 3779–3804.

82 A. Naqavi, F.-J. Haug, C. Ballif, T. Schart and H. P. Herzig, Limit of light coupling strength in solar cells, *Appl. Phys. Lett.*, 2013, **102**, 131113.

83 K. M. Ho, C. T. Chan, C. M. Soukoulis, R. Biswas and M. Sigalas, Photonic band gaps in three dimensions: New layer-by-layer periodic structures, *Solid State Commun.*, 1994, **89**, 413–416.

84 H. S. Sözüer and J. P. Dowling, Photonic band calculations for woodpile structures, *J. Mod. Opt.*, 1994, **41**, 231–239.

85 S.-Y. Lin, J. G. Fleming, D. L. Hetherington, B. K. Smith, R. Biswas, K. M. Ho, M. M. Sigalas, W. Zubrzycki, S. R. Kurtz and J. Bur, A three-dimensional photonic crystal operating at infrared wavelengths, *Nature*, 1998, **394**, 251–253.

86 O. J. Painter, A. Husain, A. Scherer, J. D. O'Brien, I. Kim and P. D. Dapkus, Room temperature photonic crystal defect lasers at near-infrared wavelengths in InGaAsP, *J. Lightwave Technol.*, 1999, **17**, 2082–2088.

87 Y. A. Vlasov, X.-Z. Bo, J. C. Sturm and D. J. Norris, On-chip natural assembly of silicon photonic bandgap crystals, *Nature*, 2001, **414**, 289–293.

88 M. Lončar, T. Yoshie, A. Scherer, P. Gogna and Y. Qiu, Low-threshold photonic crystal laser, *Appl. Phys. Lett.*, 2002, **81**, 2680–2682.

89 M. Qi, E. Lidorikis, P. T. Rakich, S. G. Johnson, J. D. Joannopoulos, E. P. Ippen and H. I. Smith, A three-dimensional optical photonic crystal with designed point defects, *Nature*, 2004, **429**, 538–542.

90 B.-S. Song, S. Noda, T. Asano and Y. Akahane, Ultra-high-Q photonic double-heterostructure nanocavity, *Nat. Mater.*, 2005, **4**, 207–210.

91 E. C. Nelson, N. L. Dias, K. P. Bassett, S. N. Dunham, V. Verma, M. Miyake, P. Wiltzius, J. A. Rogers, J. J. Coleman, X. Li and P. V. Braun, Epitaxial growth of three-dimensionally architectured optoelectronic devices, *Nat. Mater.*, 2011, **10**, 676.

92 J.-D. Chen, L. Zhou, Q.-D. Ou, Y.-Q. Li, S. Shen, S.-T. Lee and J.-X. Tang, Enhanced light harvesting in organic solar cells featuring a biomimetic active layer and a self-cleaning antireflective coating, *Adv. Energy Mater.*, 2014, DOI: 10.1002/AENM.201301777.

93 F. Boudoire, R. Toth, J. Heier, A. Braun and E. C. Constable, Photonic light trapping in self-organized all-oxide microspheroids impacts photoelectrochemical water splitting, *Energy Environ. Sci.*, 2014, DOI: 10.1039/C4EE00380B.